

PRECISE EVALUATION OF CHARACTERISTIC OF THE MULTILAYER THIN-FILM SUPERCONDUCTOR CONSISTING OF NbN AND INSULATOR ON PURE Nb SUBSTRATE

R. Katayama*, Y. Iwashita, H. Tongu, Kyoto ICR, Uji, Kyoto
A. Four, CEA/DRF/IRFU, Gif-sur-Yvette, C. Z. Antoine, CEA/IRFU, Gif-sur-Yvette
H. Hayano, T. Kubo, T. Saeki, KEK, Ibaraki, Hayato Ito, Sokendai, Ibaraki
R. Ito, T. Nagata, ULVAC, Inc, Chiba
H. Oikawa, Utsunomiya University, Tochigi

Abstract

In recent years, it has been pointed out that the maximum accelerating gradient of a superconducting RF cavity can be pushed up by coating the inner surface of the cavity with a multilayer thin-film structure that consists of alternating insulating and superconducting layers. In this structure, the principal parameter that limits the performance of the cavity is the critical magnetic field or effective H_{C1} at which vortices start penetrating into the superconductor layer, and it is predicted to depend on the combination of the film thickness. We made samples that have NbN/SiO₂ thin-film structure on pure Nb substrate with several thicknesses of NbN film deposited using DC magnetron sputtering method. Here, we report the measurement results of effective H_{C1} of the NbN sample with a thickness of 200 nm by using the third-harmonic voltage method. In addition, we report the preliminary results to evaluate the dependence of the effective H_{C1} on the thickness of the NbN film in the range 50 nm–200 nm.

INTRODUCTION

Recently, it has been pointed out that the effective H_{C1} of a superconducting RF cavity might be pushed up by coating the inner surface of the cavity with a multilayer thin-film structure that consists of alternate insulating and superconducting layers [1–3]. Hereafter, such multilayer structures on pure bulk Nb in superconducting state is referred to as S-I-S (Superconductor-Insulator-Superconductor) structure. Generally, the effective H_{C1} of a superconducting material can be evaluated by applying a sine-wave magnetic field to the material with a small coil and detecting the third-harmonic signal of the coil voltage because the third-harmonic signal occurs when the phase transition from the full Meissner state to the vortex-penetrating state happens. Hereafter, this method is called third harmonic voltage method. C. Antoine already showed that a multilayer structure on a Nb substrate has higher effective H_{C1} than that of the Nb substrate by the third-harmonic voltage method [4]. We also verified that the effective H_{C1} is enhanced for a sample that consists of NbN (200 nm) and SiO₂ (30 nm) formed on pure Nb substrate that has an RRR of >250 [5]. Our measurement result on the third harmonic measurement using AC magnetic fields less than 13 mT are reported in IPAC18 proceedings. This article

describes details of the new result to evaluate effective H_{C1} of the NbN(200 nm)/SiO₂(30 nm)/Nb sample using the AC magnetic field of the amplitude up to 44 mT. In addition, in order to evaluate the dependence of effective H_{C1} on the film thickness, this article presents the preliminary result of the measurement of effective H_{C1} of the NbN(50 nm)/SiO₂(30 nm)/Nb sample using the AC magnetic field of the amplitude up to 29 mT.

THIRD HARMONIC MEASUREMENT

For the third harmonic voltage method, an AC magnetic field at the frequency of 5 kHz is generated by a coil close to the superconducting sample and the third harmonic voltage $v_3(t) = V_3 \sin(3\omega t)$ induced in the coil is simultaneously measured [6]; ω is the frequency of a sinusoidal drive current, $I_0 \sin(\omega t)$ represents the current flowing in the coil, and V_3 is the amplitude of $v_3(t)$. If the temperature of a sample in superconducting state is being raised while amplitude of AC magnetic field H_0 is fixed, V_3 suddenly rises when H_0 exceeds the effective H_{C1} of the sample at a certain temperature. In the measurement performed at Kyoto University, H_0 is controlled by drive current I_0 , and the temperature dependence of the effective H_{C1} is estimated from the temperatures at moments when V_3/I_0 suddenly rises. Refer to [5] for details of the measurement setup and flow.

In this study, the coil magnetic field is calibrated with the third harmonic measurement result of pure bulk Nb assuming that the following function $F(T)$ represents the temperature dependence of the effective H_{C1} of pure bulk Nb.

$$F(T) = \begin{cases} 0.18 \times (1 - (T/9.2)^2) & (T < 9.2\text{K}) \\ 0 & (T > 9.2\text{K}) \end{cases} \quad (1)$$

The calibration curve obtained from this measurement is shown in Fig. 1. The vertical axis is the coil magnetic field, and the horizontal axis is the drive current amplitude I_d derived from the digitized data recorded by our measurement system.

DETAILS OF MEASUREMENT RESULT

We have tested two multilayer samples that consist of NbN and SiO₂ coated on pure bulk Nb. The pure bulk Nb

* katayama@kyticr.kuicr.kyoto-u.ac.jp

Content from this work may be used under the terms of the CC BY 3.0 licence (© 2018). Any distribution of this work must maintain attribution to the author(s), title of the work, publisher, and DOI.

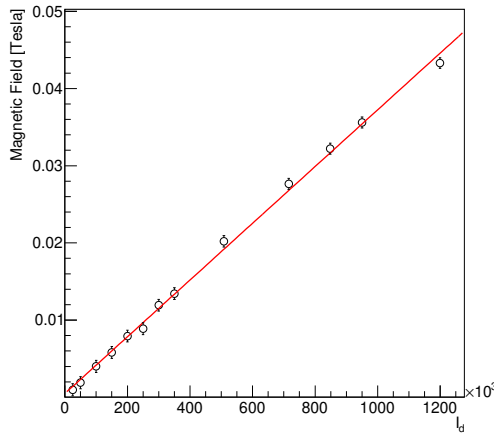


Figure 1: Calibration line of the applied magnetic field vs. the fundamental component of the coil current read I_d (arbitrary unit).

substrate of the sample is pretreated with the standard electropolishing recipe for bulk Nb cavity. Both the multilayer samples are prepared using DC magnetron sputtering technique (ULVAC, Inc.). One of the samples is a thin-film structure of 200-nm-thick NbN and 30-nm-thick SiO₂; the details of thin-film preparation are given elsewhere [7]. This sample is named as 180409-1-B. The other one is a thin-film structure of 50-nm-thick NbN and 30-nm-thick SiO₂; details of thin-film preparation are given elsewhere [8]. This sample is named as 180814-1-B. In the third harmonic measurements, the temperature ramping rates were kept at about 0.01 K/min. The systematic error is estimated to be 0.02 K in the measured temperature due to a thermal nonuniformity. It is noted that the systematic error used in this study is higher than that described in IPAC18 proceedings [5].

In our third harmonic measurements of sample No.180409-1-B, the amplitude of AC magnetic field applied to the sample was chosen to be 1.2 mT, 1.8 mT, 3.7 mT, 5.5 mT, 9.2 mT, 12.9 mT, 36.1 mT, and 44.1 mT. In this measurement, the applied magnetic field is increased by about 3 times than the measurement condition reported at IPAC18. The temperature dependence of the effective H_{C1} of the sample 180409-1-B is depicted in Fig. 2. The horizontal and vertical axes represent the temperature and the measured effective H_{C1} , respectively. The measured values of H_{C1} of pure bulk Nb sample and the effective H_{C1} of NbN(200 nm)/SiO₂(30 nm)/Nb sample are represented by the open circles and black triangles, respectively. The red curve is the theoretical curve obtained from equation (1), which is used for calibration. The green dashed curve is obtained by fitting data points of the sample of 180409-1-B in the region $T < 9.2$ K to the function (2). On the other hand, the blue one dot chain line is obtained by fitting data points of the sample of 180409-1-B in the region $T > 9.2$ K to the function (2). In this fitting, T'_C was fixed at 13.8 K, a value obtained from the measurement result of the critical

temperature of NbN film at KEK [9]. At temperatures below around 9.2 K, S-I-S structure is formed because both pure bulk Nb and NbN film are in superconducting state. Thus, the effective H_{C1} of the whole NbN/SiO₂/Nb structure in the superconducting state is expressed by the green dashed curve. On the other hand, for temperatures greater than around 9.2 K, S-I-S structure does not hold. Thus, the blue one dot chain line corresponds to the effective H_{C1} of only NbN film. As a result of fitting, $f(0)$ and T'_C , parameters of the function (2), are estimated as $(210 \pm 7) \times 10^{-3}$ and 9.21 ± 0.02 K, respectively for the green dashed curve, whereas $f(0)$ is determined as $(3.3 \pm 0.5) \times 10^{-3}$ for the blue one dot chain line. It is thus confirmed that $f(0)$ of NbN(200 nm)/SiO₂(30 nm)/Nb in the region of $T < 9.2$ K is improved by 17 % compared to that of pure bulk Nb.

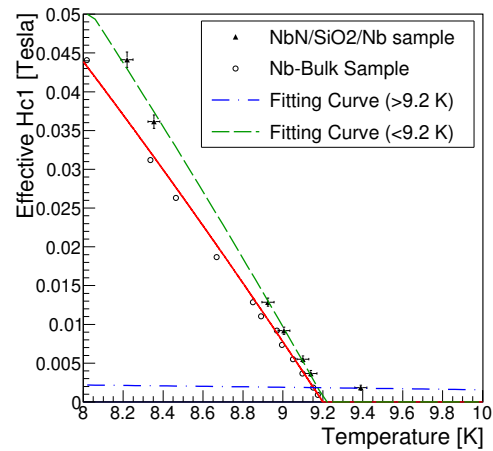


Figure 2: Comparison of measured effective H_{C1} between NbN(200 nm)/SiO₂(30 nm)/Nb and pure bulk Nb samples. The red curve represents the equation (1), which is used for calibration. The green broken line and the blue chain line are obtained by fitting data points of sample No.180409-1-B.

In our third harmonic measurements of sample No. 180814-1-B, the amplitude of AC magnetic field applied to the sample was chosen to be 14.8 mT, 22.6 mT, and 29.3 mT. The preliminary result of the temperature dependence of the effective H_{C1} of NbN(50 nm)/SiO₂(30 nm)/Nb and pure bulk Nb is shown in Fig. 3. The horizontal and vertical axes represent the temperature and the measured effective H_{C1} , respectively. The measurement result of H_{C1} of pure bulk Nb sample and the measurement result of effective H_{C1} of NbN/SiO₂/Nb sample are represented by open circles and black triangles, respectively. The red curve represents the equation (1), which is used for calibration. The green dashed curve is obtained by fitting data points of the sample of 180814-1-B in the region of $T < 9.2$ K, to the function of (2). As a result of fitting, $f(0)$ and T'_C , parameters of the function (2), are determined as $(176 \pm 16) \times 10^{-3}$ and 9.21 ± 0.06 K, respectively. The theoretical calculation of the dependence of effective H_{C1} on the film thickness is shown

in Fig. 4. It is found that the result obtained in this study is qualitatively consistent with the prediction of theory.

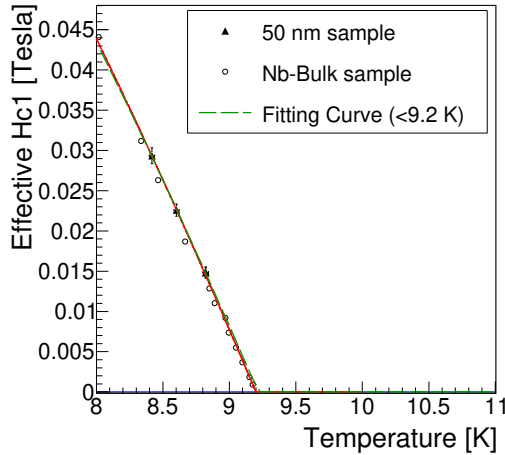


Figure 3: Comparison of measured effective H_{C1} of NbN(50 nm)/SiO₂(30 nm)/Nb and pure bulk Nb samples. The red curve represents the equation (1) used for calibration. The green broken line is obtained by fitting the data points of sample No.180814-1-B.

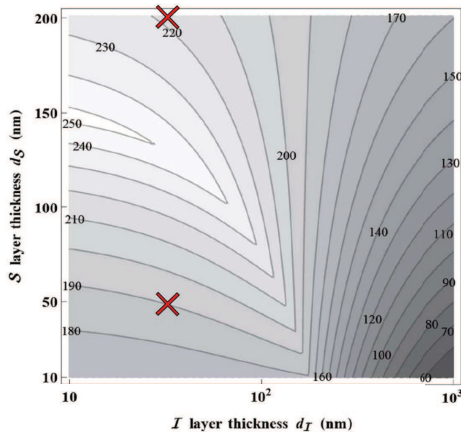


Figure 4: Theoretical calculation of the effective H_{C1} for NbN-I-Nb at $T = 2$ K (the image is cited from [3] and partially changed). The horizontal and vertical axes represent the thickness of the insulating layer and that of the superconducting layer, respectively. Each value shown in the contour plot denotes the effective H_{C1} that depends on the film thickness, and each cross in the figure corresponds to the test point in this study.

SUMMARY AND FUTURE PROSPECT

We evaluated the temperature dependence of effective H_{C1} of a sample having S-I-S structure that consists of NbN superconducting layer and SiO₂ insulating layer (30 nm) formed on pure bulk Nb. The measurement result clearly showed that the effective H_{C1} of pure bulk Nb improved after NbN/SiO₂ film coating, whereas effective H_{C1} changed

depending on the film thickness. As a future prospect, in order to ensure the reproducibility, we plan to test the samples, which were fabricated in the same sputtering method, by other experimental setups at KEK [10] and Saclay [4]. In addition, by using the NbN samples with film thickness of 100 nm, 150 nm, 250 nm, 300 nm, and 400 nm that we have already prepared [8], we would like to clarify the dependence of effective H_{C1} on the film thickness.

ACKNOWLEDGMENTS

This work is supported by JSPS KAKENHI Grant Number JP17H04839, JSPS KAKENHI Grant Number JP26600142, Photon and Quantum Basic Research Coordinated Development Program of MEXT, Japan, Center of Innovation (COI) Program, Japan-US Research Collaboration Program, and the Collaborative Research Program of Institute for Chemical Research, Kyoto University (2016-8).

APPENDIX

In this paper, the following function is used in Fig. 2 and Fig. 3:

$$f(T) = f(0) \times \left(1 - (T/T'_C)^2\right) \quad (2)$$

REFERENCES

- [1] A. Gurevich, "Enhancement of rf breakdown field of superconductors by multilayer coating", *Appl. Phys. Lett.* 88, 012511 (2006).
- [2] T. Kubo, *et al.*, "Radio-frequency electromagnetic field and vortex penetration in multilayered superconductors", *Appl. Phys. Lett.* 104, 032603 (2014).
- [3] T. Kubo, "Multilayer coating for higher accelerating fields in superconducting radio-frequency cavities: a review of theoretical aspects", *Supercond. Sci. Technol.* 30, 023001 (2017).
- [4] C. Z. Antoine, M. Aburas, A. Four, *et al.*, "Progress on characterization and optimization of multilayers", in *Proc. SRF'17*, Lanzhou, China, Jul. 2017. doi:10.18429/JACoW-SRF2017-TUYBA01
- [5] R. Katayama, *et al.*, "Evaluation of superconducting characteristics on the thin-film structure by NbN and Insulator coatings on pure Nb substrate", in *Proc. IPAC'18*, Vancouver, Canada, Apr. 2018. doi:10.18429/JACoW-IPAC2018-THPAL015
- [6] Y. Mawatari, *et al.*, "Critical current density and third-harmonic voltage in superconducting films", *Appl. Phys. Lett.* 81, 2424 (2002).
- [7] R. Ito, T. Nagata, *et al.*, "Development of Coating Technique for Superconducting Multilayered Structure", in *Proc. IPAC'18*, Vancouver, Canada, Apr. 2018. doi:10.18429/JACoW-IPAC2018-THPML120
- [8] R. Ito, T. Nagata, *et al.*, "Construction of Thin-film Coating System Toward the Realization of Superconducting Multilayered Structure", presented at LINAC'18, Beijing, China, Sept. 2018, paper TUP0050, this conference.

Content from this work may be used under the terms of the CC BY 3.0 licence (© 2018). Any distribution of this work must maintain attribution to the author(s), title of the work, publisher, and DOI.

- [9] H. Ito, *et al.*, “Lower Critical Field Measurement System of Thin Film Superconductor”, in *Proc. IPAC’18*, Vancouver, Canada, Apr. 2018. doi:10.18429/JACoW-IPAC2018-THPAL105
- [10] H. Ito, *et al.*, “Lower Critical Field Measurement of Thin Film Superconductor”, presented at LINAC’18, Beijing, China, Sept. 2018, paper TUPO66, this conference.